A CASSCF and CCI Study of the Photochemistry of $HCo(CO)_4$

Alain Veillard* and Alain Strich

Contribution from E.R. No. 139 du CNRS, Laboratoire de Chimie Quantique, Institut Le Bel, 4 rue Bl. Pascal, 67000 Strasbourg, France. *Received October 23, 1987*

Abstract: The photochemistry of $HCo(CO)_4$ has been studied theoretically through ab initio contracted configuration interaction (CCI) calculations of the potential energy curves which connect the ground and low excited states of $HCo(CO)_4$ with the ground and excited states of the products:

$$HCo(CO)_4 \xrightarrow{h\nu} H^{\bullet} + {}^{\bullet}Co(CO)_4 \quad (1)$$

$$HCo(CO)_4 \xrightarrow{h\nu} CO + HCo(CO)_3 \quad (2)$$

The calculations were carried out for the dissociation of the axial ligands (hydrogen or carbonyl) under C_{3v} constraint, with a basis set which is at least of double-ζ quality. The CCI calculations, which correlate the metal 3d electrons and the two electrons of the Co–H bond, are based on a CASSCF reference wave function with six electrons in six active orbitals ($3d_\delta$, $4d_\delta$, σ_{Co-H}, and σ^*_{Co-H}), optimized for the $^3A_1$ $\sigma \rightarrow \sigma^*$ state. It is proposed that the photochemistry of $HCo(CO)_4$ occurs through excitation to the ^1E $d_\delta \rightarrow \sigma^*$ state followed by intersystem crossing to the $^3A_1$ state. From there the molecule has a choice between three different channels corresponding respectively to dissociation into the products H + $Co(CO)_4$ in their ground state or CO + $HCo(CO)_3$ in the excited states $^3A_1$ or ^3E. It is predicted that chemiluminescence should be observed for the photodecarbonylation in the gas phase. It is proposed, on an analogy ground, that the dissociative character of the $^3A_1$ curve with respect to the carbonyl loss explains the occurrence of two primary photoprocesses for $Mn_2(CO)_{10}$ at 337 nm, one of metal–metal bond cleavage and the other of dissociative loss of CO.

Although there is an extensive photochemistry of organometallic compounds,[1] the mechanism of the primary photochemical reactions of organometallics is poorly understood.[1,2] "One unfortunate characteristic of much of organometallic photochemistry is a relative absence of detailed mechanistic information. Without such information the systematic and rationally planned use of photochemical techniques is left largely to chance."[2] Two important classes of photochemical reactions in organometallic chemistry are the homolysis of a bond originating from the metal atom (metal–hydrogen or metal–alkyl or metal–metal)

$$L_nM\text{–}X \xrightarrow{h\nu} L_nM^{\bullet} + X^{\bullet} \quad (X = H, R, ML_n) \quad (3)$$

and the heterolytic loss of a carbonyl ligand

$$L_nM\text{–}CO \xrightarrow{h\nu} L_nM + CO \quad (4)$$

A number of organometallics, upon irradiation, undergo both photochemical processes, either at a unique wavelength or at different wavelengths. Typical examples include the hydrides $HCo(CO)_4$[3,4] and $HMn(CO)_5$[5,6]

$$HCo(CO)_4 \xrightarrow[254\text{ nm}]{h\nu} H^{\bullet} + {}^{\bullet}Co(CO)_4 \quad (5)$$

$$\xrightarrow[254\text{ nm}]{h\nu} CO + HCo(CO)_3 \quad (6)$$

$$HMn(CO)_5 \xrightarrow[193\text{ nm}]{h\nu} H^{\bullet} + {}^{\bullet}Mn(CO)_5 \quad (7)$$

$$\xrightarrow[229\text{ nm}]{h\nu} CO + HMn(CO)_3 \quad (8)$$

and the dimer $Mn_2(CO)_{10}$

$$Mn_2(CO)_{10} \xrightarrow[337\text{ nm}]{h\nu} 2Mn(CO)_5 \quad (9)$$

$$\xrightarrow[337\text{ nm}]{h\nu} CO + Mn_2(CO)_9 \quad (10)$$

Chart I

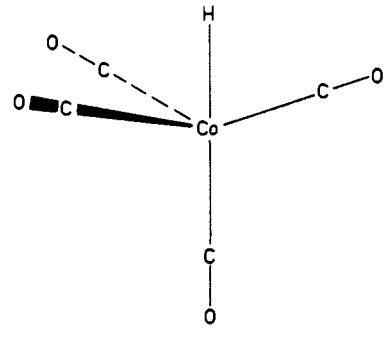

Scheme I

In order to understand the photochemistry of these systems, one needs some knowledge of their excited states and of the corresponding potential energy surfaces. For $HCo(CO)_4$ we have previously studied[7] reaction 5 through ab initio configuration interaction (CI) calculations of the potential energy curves which connect the ground and lowest excited states of $HCo(CO)_4$ with the states of the products H + $Co(CO)_4$. We proposed that the photolysis of the Co–H bond occurs through excitation to a singlet state followed by intersystem crossing to the $^3A_1$ $\sigma \rightarrow \sigma^*$ state (σ and σ^* denote the MOs which are respectively bonding and antibonding with respect to the metal–hydrogen bond) with subsequent dissociation to the products of the reaction along this $^3A_1$ potential energy curve. In these CI calculations, the $\sigma \rightarrow \sigma^*$ $^3A_1$ state was calculated at about 41 000 cm^{-1}, the lowest singlet state being a $d_\delta \rightarrow \sigma^*$ ^1E state at about 47 000 cm^{-1} (the electronic spectrum of $HCo(CO)_4$ shows a broad band at 44 000 cm^{-1})[4] (in what follows, the notation σ, π, δ refers to the C_3 axis taken as the O_z axis with d_δ being d_{xy}, $d_{x^2-y^2}$ and d_π being d_{xz}, d_{yz}).

(1) Geoffroy, G. L.; Wrighton, M. S. *Organometallic Photochemistry*; Academic: New York, 1979.
(2) Meyer, T. J.; Caspar, J. V. *Chem. Rev.* **1985**, *85*, 187.
(3) Sweany, R. L. *Inorg. Chem.* **1980**, *19*, 3512.
(4) Sweany, R. L. *Inorg. Chem.* **1982**, *21*, 752.
(5) Rest, A. J.; Turner, J. J. *J. Chem. Soc., Chem. Commun.* **1969**, *375*.
(6) Church, S. P.; Polyakoff, M.; Timmey, J. A.; Turner, J. J. *Inorg. Chem.* **1983**, *22*, 3259.
(7) Daniel, C.; Hyla-Kryspin, I.; Demuynck, J.; Veillard, A. *Nouv. J. Chim.* **1985**, *9*, 581.

0002-7863/88/1510-3793$01.50/0

Scheme II

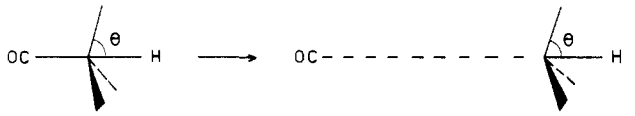

Besides theoretical studies of the ground state,[8-13] another study,[14] based on SCF-Xα-SW calculations, dealt with the excited states of $HCo(CO)_4$ and the conclusions reached were somewhat different from ours.[7] In this study, the state $^3A_1$ corresponding to the $\sigma \rightarrow \sigma^*$ excitation is not mentioned in the calculation of the transition energies, with the photochemical reaction being assigned to a $e \rightarrow a_1$ transition (mostly $d \rightarrow \sigma^*$ in character).

We present here a more extensive investigation of the potential energy surfaces for the two photochemical processes of $HCo(CO)_4$ corresponding to the dissociation of the Co–H bond and to the loss of a carbonyl ligand, through more accurate CI calculations based on CASSCF reference wave functions.

Method and Computational Details

$HCo(CO)_4$ (Chart I) is a distorted trigonal bipyramid with C_{3v} symmetry.[15] Potential energy curves were computed for two reaction paths corresponding respectively to the dissociation of the Co–H bond (Scheme I) and to the loss of the axial carbonyl ligand (Scheme II), with the following assumptions:

(i) C_{3v} symmetry is retained along the reaction path. Support for this assumption comes from the fact that of the different geometries investigated for $Co(CO)_4$ (at the SCF level) and for $HCo(CO)_3$ (at the CI level) the lowest in energy was of C_{3v} symmetry.[7]

(ii) The bond lengths were kept constant and equal to the experimental values[15] (except for the bond which dissociates).

(iii) During the dissociation of the Co–H bond (Scheme I), the angle τ was kept equal to 100° for all the points along the reaction path (the experimental value[15] for $HCo(CO)_4$ being 99.7° with the value optimized for $Co(CO)_4$ at the SCF level being close to 100°[7]).

(iv) The angle θ (Scheme II) was optimized at the SCF level along the reaction path corresponding to the loss of a carbonyl ligand (the experimental value of θ being 80° for $HCo(CO)_4$ versus an optimized value of 90° for $HCo(CO)_3$ at the CI level[16]).

The following basis sets were used: for the Co atom a (15,11,6) set contracted to [9,6,3],[17] for the first-row atoms a (10,6) set contracted to [4,2],[20] and for hydrogen a (6,1) set contracted to [3,1].[21] This basis set is triple-ζ for the 1s shell of hydrogen and for the 3d and 4s shells of cobalt, otherwise it is double-ζ.

The CASSCF (complete active space SCF) method[22] was used to obtain reference wave functions and orbitals. These CASSCF calculations were followed by contracted CI (CCI) calculations.[23] The rigorous way to calculate potential energy surfaces consists of carrying out for each electronic state a CASSCF calculation followed by a contracted CI calculation.[24] However this procedure was too expensive for the studies reported here. The approach that we have used consists of performing a CASSCF calculation for a particular state and using this CASSCF reference wave function for the CCI calculations of all the states of interest. The choice of this particular state was dictated by the following considerations. The ground state is not the best candidate, since the CCI calculations would be biased in favor of this state and would tend to overestimate the excitation energies.[25] Since our interest will center mostly on the excited states $d_\delta \rightarrow \sigma^*$ $^{1,3}E$ and $\sigma \rightarrow \sigma^*$ $^3A_1$ which both have a σ^* orbital with an occupation number close to one, the CASSCF calculations were carried out for the state $\sigma \rightarrow \sigma^*$ $^3A_1$. Ideally, this CASSCF calculation should include ten active orbitals: the 3d orbitals, the 4d orbitals which correlate them, and the σ and σ^* orbitals. However, the cost in terms of computation was too high (mostly due to the fact that the corresponding root was not the lowest one). We checked that excluding the $3d_\pi$ and $4d_\pi$ orbitals from the active set represents a reasonable approximation by carrying out two CASSCF calculations for the ground-state $^1A_1$, one (denoted 10a10e, standing for 10 electrons in 10 active orbitals) with and the other (denoted 6a6e) without the d_π orbitals. The corresponding wave functions were used as reference wave functions in CCI calculations of the ground and excited states of $HCo(CO)_4$, and it turned out that the corresponding excitation energies differ by at most 2600 cm^{-1}. Since our goal is to obtain a qualitative understanding of the mechanism of these photochemical reactions rather than an accurate description of the potential energy surfaces, we felt that the approximation of excluding the d_π orbitals from the CASSCF active space was reasonable.

For each electronic state, two CCI calculations were performed. The first one has only one reference configuration whereas the second one is a multireference calculation. The reference configurations of the latter are the configurations which appear with a coefficient greater than 0.08 in the wave function from the former. The number of reference configurations selected in this way was between 3 and 5. In what follows, we discuss only the results from the multireference CCI calculations. Ten electrons were correlated in these calculations (the 3d electrons and those of the Co–H bond). The calculations included single and double excitations to all virtual orbitals except the counterparts of the carbonyl 1s and of the metal 1s, 2s, and 2p orbitals. For $HCo(CO)_4$, the number of configurations ranged from 183 000 to 509 000, but this number was reduced to at most a few thousands by the contraction.

The integral calculations were carried out with the system of programs ARGOS,[26] with all the calculations performed in C_s symmetry.

Table I. CASSCF and CCI Total Energies for the Ground State $^1A_1$ and for the Excited State $^3A_1$ of $HCo(CO)_4$

state	principal configuration	total energy (au)	
$^1A_1$	$d_\pi^4 d_\delta^4 \sigma^2$	CASSCF 6a6e	−1832.6085
		CASSCF 10a10e	−1832.7549
		CCI	−1832.7318 (4)[a-c]
$^3A_1$	$d_\pi^4 d_\delta^4 \sigma^1 \sigma^{*1}$	CASSCF 6a6e	−1832.4101
		CCI	−1832.5598 (3)[d]

[a] With the CASSCF 6a6e wave function optimized for the $^1A_1$ state as reference wave function. [b] The number in parentheses denotes the number of reference configurations. [c] The CCI total energy is higher than the CASSCF 10a10e total energy since the CCI calculation includes only single and double excitations whereas the CASSCF calculation includes all excitations within the active space. [d] With the CASSCF 6a6e wave function optimized for the $^3A_1$ state as reference wave function.

Table II. Calculated CCI Excitation Energies (cm^{-1}) for $HCo(CO)_4$

	one-electron excitation in the principal configuration	
$^1A_1 \rightarrow {}^1E$	$d_\delta \rightarrow \sigma^*$	36 000[a]
$^1A_1 \rightarrow {}^3A_1$	$\sigma \rightarrow \sigma^*$	34 600
$^1A_1 \rightarrow {}^3E$	$d_\delta \rightarrow \sigma^*$	25 900

[a] Symmetry allowed.

Results and Discussion

$HCo(CO)_4$. The total energies from the CASSCF and the corresponding CCI calculations are reported in Table I for the

(8) Fonnesbech, N.; Hjortkjaer, J.; Johansen, H. *Int. J. Quantum Chem.* **1977**, *12* (Supp. 2), 95.
(9) Grima, J. Ph.; Choplin, F.; Kaufmann, G. *J. Organomet. Chem.* **1977**, *129*, 221.
(10) Pensak, D. A.; McKinney, R. J. *Inorg. Chem.* **1979**, *18*, 3407.
(11) Bellagamba, V.; Ercoli, R.; Gamba, A.; Suffriti, G. B. *J. Organomet. Chem.* **1980**, *190*, 381.
(12) Boudreaux, E. A. *Inorg. Chim.* Acta **1984**, *82*, 183.
(13) Antolovic, D.; Davidson, E. R. *J. Am. Chem. Soc.* **1987**, *109*, 977.
(14) Eyermann, C. J.; Chung-Phillips, A. *J. Am. Chem. Soc.* **1984**, *106*, 7437.
(15) McNeill, E. A.; Schöler, F. R. *J. Am. Chem. Soc.* **1977**, *99*, 6243.
(16) Veillard, A., unpublished results.
(17) This basis set is made from the (14,9,5) basis of Wachters[18] by adding an additional s function (exponent 0.3218), two diffuse p functions, and one diffuse d function. All these exponents were chosen according to the even-tempered criterion of Raffenetti et al.[19]
(18) Wachters, A. J. H. *J. Chem. Phys.* **1970**, *52*, 1033.
(19) Raffenetti, R. C.; Bardo, R. D.; Ruedenberg, K. In *Energy, Structure and Reactivity*; Smith, D. W., Mc Rae, W. B., Eds.; Wiley: New York, 1973; p 164.
(20) Huzinaga, S. *Approximate atomic functions*; Technical Report, University of Alberta, Alberta, 1971.
(21) Huzinaga, S. *J. Chem. Phys.* **1965**, *42*, 1293.
(22) Siegbahn, P. E. M.; Almlof, J.; Heiberg, A.; Roos, B. O. *J. Chem. Phys.* **1981**, *74*, 2384.
(23) Siegbahn, P. E. M. *Int. J. Quantum Chem.* **1983**, *23*, 1869.
(24) See for instance: Matos, J. M. O.; Roos, B.; Malmqvist, P. A. *J. Chem. Phys.* **1987**, *86*, 1458.
(25) Another argument against the use of a CASSCF wave function optimized for the ground state is that, in the corresponding calculation, the σ^* orbital, with an occupation number close to zero, serves mostly to correlate the σ orbital and as such is not very appropriate to describe the excited states where this orbital has an occupation number close to one.
(26) Pitzer, R. M. *J. Chem. Phys.* **1973**, *58*, 3111.

Table III. CCI Energy Values (au) Along the Potential Energy Curves for the Reaction $HCo(CO)_4 \rightarrow H + Co(CO)_4$, as a Function of the Distance Co–H[30]

	1.556 Å	2.0 Å	2.5 Å	3.0 Å	50.0 Å
^1E	−1832.55363	−1832.57144	−1832.58173	−1832.58670	−1832.60108
$^3A_1$	−1832.55984	−1832.63030	−1832.65179	−1832.65843	−1832.66102
^3E	−1832.59946	−1832.60656	−1832.59608	−1832.59467	−1832.60103
$^1A_1$	−1832.71767	−1832.69175	−1832.66310	−1832.65839	−1832.66091

Table IV. CCI Energy Values (au) Along the Potential Energy Curves for the Reaction $HCo(CO)_4 \rightarrow CO + HCo(CO)_3$, as a Function of the Distance $Co–C_{axial}$

	1.764 Å	2.1 Å	2.5 Å	3.0 Å	50.0 Å
$^3A_1$	−1832.55984	−1832.59128	−1832.60879	−1832.62067	−1832.61559
^3E	−1832.59946	−1832.62430	−1832.63127	−1832.63839	−1832.63816
$^1A_1$	−1832.71767	−1832.72416	−1832.71608	−1832.70777	−1832.69634

ground state $^1A_1$ and the excited state $^3A_1$ of $HCo(CO)_4$ (the reader is referred to previous studies[13,27] for a qualitative description of the molecular orbitals of $HCo(CO)_4$). Excitation energies to the lowest excited states of $HCo(CO)_4$ are given in Table II. We have previously shown[7] that the ^1E $d_\delta \rightarrow \sigma^*$ state is the lowest excited singlet and this has been confirmed by exploratory CASSCF and CCI calculations. No attempt has been made to compute higher excited states (resulting from the excitations $d_\pi \rightarrow \sigma^*$, $3d \rightarrow 4d$, and $d \rightarrow \pi^*_{CO}$). It has been shown for $HMn(CO)_5$[28] that this method yields reasonable excitation energies, with errors which probably do not exceed 0.5 eV.[29] The experimental spectrum of $HCo(CO)_4$[4] shows an intense band centered at 44 000 cm^{-1} and corresponding certainly to a $d \rightarrow \pi^*_{CO}$ charge-transfer transition. The absorption starts at about 36 000 cm^{-1}, in good agreement with the value calculated for the excitation energy to the state ^1E $d_\delta \rightarrow \sigma^*$ with this $d_\delta \rightarrow \sigma^*$ transition probably buried under the more intense CT transition in the experimental spectrum.

The Potential Energy Curves for Hydrogen Dissociation. The CCI energies for the potential energy curves corresponding to the dissociation of the Co–H bond under C_{3v} constraint are reported in Table III. The corresponding potential energy curves are shown in Figure 1. From the values of Table III, the bond dissociation energy for the Co–H bond is 35.6 kcal/mol. A more realistic value of 44.5 kcal/mol is obtained when the CCI energy values are based on a CASSCF reference wave function optimized for the ground state $^1A_1$. A measurement of this bond energy yielded a value of 57 kcal/mol.[31] Previous theoretical estimates have produced values of 64 kcal/mol at the EHT level[32] and 55 kcal/mol from a Hartree–Fock–Slater calculation.[33] We have not attempted to optimize the Co–H bond length in $HCo(CO)_4$ (since we have used experimental values for the other bond lengths).[34] This may partly explain why our best value of 44 kcal/mol is slightly lower than the other values from the literature.

In agreement with our previous results,[7] the ^3E curve does not show any dissociative character, whereas the ^1E curve is only weakly dissociative. The undulatory character of the ^3E curve does not seem to be a consequence of numerical inaccuracies since

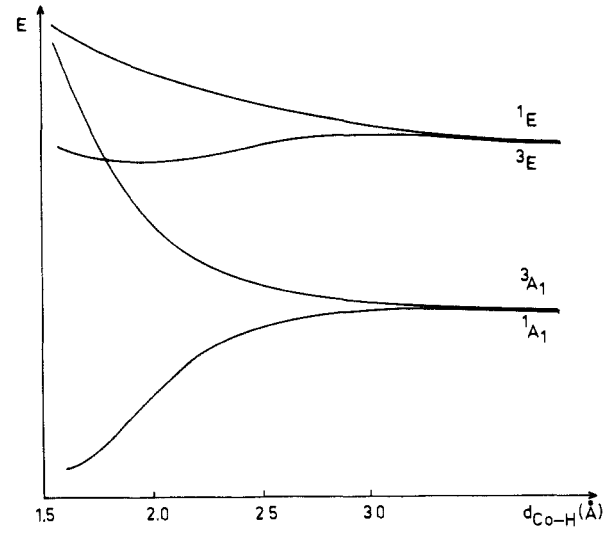

Figure 1. CCI potential energy curves for the dissociation of the Co–H bond in $HCo(CO)_4$.

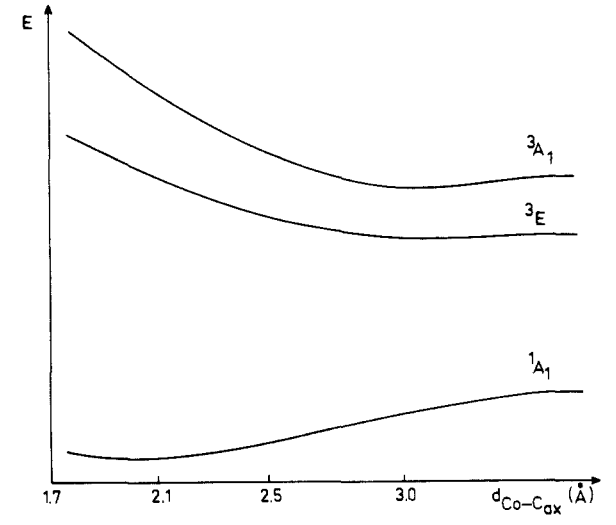

Figure 2. CCI potential energy curves for the dissociation of the $Co–C_{ax}$ bond in $HCo(CO)_4$.

a similar pattern may be found in the $^2\Sigma^-$ potential energy curve of CH.[36]

The Potential Energy Curves for the Loss of the Axial Carbonyl Ligand. The CCI energies for the potential energy curves corresponding to the loss of the axial carbonyl ligand are reported in Table IV. The corresponding potential energy curves are shown in Figure 2 (the potential energy curve for the excited state $d_\delta \rightarrow \sigma^*$ ^1E has not been computed since it does not seem to play

(27) Elian, M.; Hoffmann, R. *Inorg. Chem.* **1975**, *14*, 1058.
(28) Veillard, A.; Strich, A.; Daniel, C.; Siegbahn, P. E. M. *Chem. Phys. Lett.* **1987**, *141*, 329.
(29) We believe that the results of Table II are slightly underestimated as a consequence of a less accurate description of the ground state.[28]
(30) At 3.0 Å, the energy value of Table III for the ground state $^1A_1$ (−1832.6584 au) shows an anomalous behavior since it is higher than the value at 50 Å (−1832.6610 au), corresponding to an infinite separation. This is a consequence of the use of a reference wave function optimized for the $^3A_1$ state, since the correct behavior is obtained with the use of a reference wave function optimized for the $^1A_1$ state (yielding a CCI energy of −1832.6613 au). The $^1A_1$ curve of Figure 1 has been corrected for this anomaly.
(31) Ungvary, F. *J. Organomet. Chem.* **1972**, *36*, 363.
(32) McKinney, R. J.; Pensak, D. A. *Inorg. Chem.* **1979**, *18*, 3413.
(33) Ziegler, T.; Tschinke, V.; Becke, A. *J. Am. Chem. Soc.* **1987**, *109*, 1351.
(34) For $H_2Fe(CO)_4$, the optimized Fe–H bond length is slightly longer than the experimental value (1.60 Å versus 1.56 Å)[35].
(35) Dedieu, A.; Nakamura, S.; Sheldon, J. C. *Chem. Phys. Lett.* **1987**, *141*, 323.
(36) van Dishoeck, E. F. *J. Chem. Phys.* **1986**, *86*, 196.

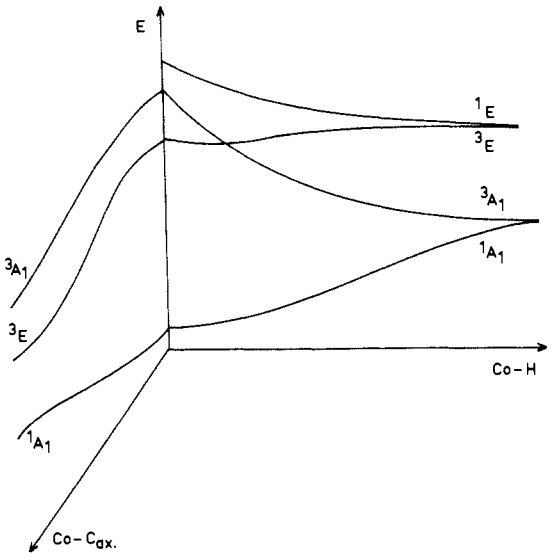

Figure 3. Potential energy surfaces corresponding to the loss of hydrogen and axial carbonyl ligand in $HCo(CO)_4$.

a role in the photochemistry of $HCo(CO)_4$). One significant feature of Table IV and Figure 2 is the presence of a minimum in the vicinity of 2.0 Å on the potential energy curve for the ground state $^1A_1$, to be contrasted with the experimental bond length of 1.764 Å.[15] It is well known that optimization of the geometry in metal carbonyls at the SCF level produces metal–carbon bond lengths which are too long.[35,37,38] This is corrected by CASSCF or CI calculations mostly through the correlation of the d_π electrons.[35,38] Although the d_π electrons are correlated in the present CCI calculations, they are not correlated in the CASSCF calculation. It is possible that the CASSCF reference wave function is not very well suited for correlating the d_π electrons and this may result in the presence of a minimum around 2.0 Å in the CCI $^1A_1$ potential energy curve. The bond dissociation energy for the Co–C bond, based on the values of Table IV, is 17.5 kcal/mol. A value of 21.9 kcal/mol is obtained from the CCI calculations with a CASSCF reference wave function optimized for the ground state. In the absence of experimental value, we note that this result is significantly lower than the bond dissociation energy of $Cr(CO)_6$ and of $Fe(CO)_5$ (respectively in the range 35–39 and 42–44 kcal/mol[39]). The large trans influence[40] of the hydrogen ligand, which weakens this bond, possibly accounts for part of the difference (although it does not explain that the axial bond length is experimentally shorter than the equatorial one,[15] as pointed out by one referee). On the other hand, there are two main causes of error in our calculation. One is that the 5σ orbital of the leaving carbonyl has not been correlated and this probably results in a binding energy which is underestimated.[41] Another possible cause, already mentioned, is that the d_π orbitals, which were not correlated in the CASSCF calculation, may not be very well suited for a description of the correlation effects associated with the d_π electrons (for the importance of d_π correlation effects on the description of the metal–carbonyl bond, see ref 38, 45–48).

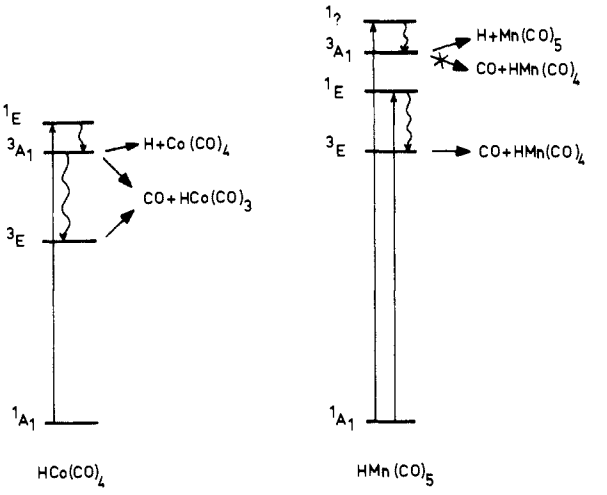

Figure 4. State diagrams for $HCo(CO)_4$ and $HMn(CO)_5$ (based on this work and on the results of ref 28).

One will notice that the potential energy curves for the two excited states ^3E $d_\delta \rightarrow \sigma^*$ and $^3A_1$ $\sigma \rightarrow \sigma^*$ are dissociative with respect to the axial carbonyl ligand, with the $^3A_1$ curve showing a shallow minimum around 3.0 Å.

The Potential Energy Surfaces for $HCo(CO)_4$ and the Photochemistry of $HCo(CO)_4$. From the two sets of potential energy curves shown in Figures 1 and 2, one can infer the shape of the potential energy surfaces (PES) of $HCo(CO)_4$ for hydrogen and carbonyl losses. These qualitative PES are represented in Figure 3, one important feature being the intersection of the $^3A_1$ and the ^3E surfaces. The PES of Figure 3 form the basis for a qualitative understanding of the photochemistry of $HCo(CO)_4$. We propose that irradiation at the experimental wavelength of 254 nm or 39 400 cm^{-1} brings the molecule into the ^1E state corresponding to the $d_\delta \rightarrow \sigma^*$ excitation (calculated at 36 000 cm^{-1}). The close proximity of the two states ^1E and $^3A_1$ (with a calculated separation of 1600 cm^{-1}) makes intersystem crossing to the $^3A_1$ $\sigma \rightarrow \sigma^*$ state an easy process[49] (intersystem crossing is a well-documented process in the photochemistry of organometallics, see for instance ref 50–53). From there the molecule may evolve along three different channels corresponding to (i) the dissociation of the Co–H bond along the $^3A_1$ curve, with formation of the products H and $Co(CO)_4$ in their ground state; (ii) the loss of a carbonyl ligand along the $^3A_1$ curve, forming the products CO and $HCo(CO)_3$, the latter in the excited state $^3A_1$ and (iii) the formation of the products CO and $HCo(CO)_3$, the latter in the excited state ^3E, by crossing from the $^3A_1$ to the ^3E surface. Thus, the PES of Figure 3 account for the occurrence of different reactive channels in the photochemistry of $HCo(CO)_4$. We predict that chemiluminescence should be observed for the photochemical decarbonylation in the gas phase (chemiluminescence has been predicted and reported experimentally for the photodecarbonylation of $Ni(CO)_4$.[50,54])

It may be worthwhile to compare the photochemistry of $HCo(CO)_4$ and of $HMn(CO)_5$, since hydrogen and carbonyl losses occur at the same wavelength for the former but at different wavelengthes for the latter. In the absence of PES for $HMn(CO)_5$, any rationale should be viewed as tentative. Since the metal–hydrogen bond energy is practically the same for these two systems[33] with metal–carbonyl bond energies probably similar,[39] an

(37) Demuynck, J.; Strich, A.; Veillard, A. *Nouv. J. Chim.* **1977**, *1*, 217.
(38) Lüthi, H. P.; Siegbahn, P. E. M.; Almlöf, J. *J. Phys. Chem.* **1985**, *89*, 2156.
(39) Ziegler, T.; Tschinke, V.; Ursenbach, C. *J. Am. Chem. Soc.* **1987**, *109*, 4825 and references therein.
(40) Huheey, J. E. *Inorganic Chemistry*, 2nd ed.; Harper and Row; New York, 1978; pp 489–498.
(41) In the simple boron adducts like BH_3NH_3, BH_3PH_3, and BH_3CO, correlation energy makes a significant contribution (up to 12 kcal/mol) to the binding energy of the dative bond.[42–44]
(42) Ahlrichs, R.; Koch, W. *Chem. Phys. Lett.* **1978**, *53*, 341.
(43) Redmon, L. T.; Purvis, G. D.; Bartlett, R. J. *J. Am. Chem. Soc.* **1979**, *101*, 2856.
(44) Zirz, C.; Ahlrichs, R. *J. Chem. Phys.* **1981**, *75*, 4980.
(45) Bagus, P. S.; Roos, B. O. *J. Chem. Phys.* **1981**, *75*, 5961.
(46) Moncrieff, D.; Ford, P. C.; Hillier, I. H.; Saunders, V. R. *J. Chem. Soc., Chem. Commun.* **1983**, 1108.
(47) Blomberg, M. R. A.; Brandemark, U. B.; Siegbahn, P. E. M.; Mathisen, K.; Karlstrom, G. *J. Phys. Chem.* **1985**, *89*, 2171.
(48) Rohlfing, C. M.; Hay, P. J. *J. Chem. Phys.* **1985**, *83*, 4641.
(49) Turro, N. J. *Modern Molecular Photochemistry*; Benjamin: Menlo Park, CA, 1978.
(50) Daniel, C.; Benard, M.; Dedieu, A.; Wiest, R.; Veillard, A. *J. Phys. Chem.* **1984**, *88*, 4805.
(51) Seder, T. A.; Ouderkirk, A. J.; Weitz, E. *J. Chem. Phys.* **1986**, *85*, 1977.
(52) Demas, J. N.; Taylor, D. G. *Inorg. Chem.* **1979**, *18*, 3177.
(53) Milder, S. J.; Kliger, D. S. *J. Phys. Chem.* **1985**, *89*, 4170.
(54) Rösch, N.; Jorg, H.; Kotzian, M. *J. Chem. Phys.* **1987**, *86*, 4038.

explanation for their different behavior must be found in the electronic states of the parent molecules, which are represented in Figure 4. The two molecules differ in the relative order of the two states $^3A_1$ and ^1E. In $HCo(CO)_4$, with the ^1E state above the $^3A_1$ state, excitation to the ^1E level leads subsequently to the $^3A_1$ and ^3E states and from there to the two reactive channels. In $HMn(CO)_5$, excitation into the ^1E level can only lead to the ^3E state and to decarbonylation. The $^3A_1$ state is reached through another singlet state (unidentified so far)[28] with subsequent hydrogen loss. Since no carbonyl loss has been reported under photolysis of $HMn(CO)_5$ at 193 nm,[6] it seems that the loss of a carbonyl does not occur for $HMn(CO)_5$ along the $^3A_1$ PES. Dynamical factors (which are beyond the scope of this work) may also play some role in understanding the photochemistry of these two molecules.

Finally, the results obtained for $HCo(CO)_4$ may help to understand the photochemistry of $Mn_2(CO)_{10}$, although there are some obvious differences (for instance the $^{1,3}A_1$ $\sigma \rightarrow \sigma^*$ states in $Mn_2(CO)_{10}$ are found at lower energies with the $^1A_1$ state located at 29 700 cm^{-1})[55] (in $Mn_2(CO)_{10}$ σ and σ^* denote the MOs corresponding to the metal–metal bond). The dissociative character of the $^3A_1$ curve with respect to the carbonyl loss which we have found for $HCo(CO)_4$ may also be present for $Mn_2(CO)_{10}$. This would explain the occurrence of two primary photoprocesses for $Mn_2(CO)_{10}$ at 337–350 nm,[56,57] with the molecule undergoing either the homolysis of the metal–metal bond (reaction 9) or the loss of a carbonyl ligand (reaction 10) on the $^3A_1$ surface after intersystem crossing from the $^1A_1$ to the $^3A_1$ state.[2,58]

Conclusion

Potential energy curves corresponding to the photolysis of the Co–H bond and to the loss of the axial carbonyl ligand have been computed for the ground and excited states of $HCo(CO)_4$ from CASSCF and CCI calculations. The shape of the corresponding PES has been deduced. A *qualitative* mechanism has been proposed for the photochemistry of $HCo(CO)_4$ at 254 nm, which may be summarized as follows: the molecule, first excited to the ^1E $d_\delta \rightarrow \sigma^*$ state, reaches the state $^3A_1$ $\sigma \rightarrow \sigma^*$ through intersystem crossing, and from the state $^3A_1$, the molecule may evolve along different channels, corresponding to the dissociation of the Co–H bond along the $^3A_1$ curve or to the loss of a carbonyl ligand along the $^3A_1$ or the ^3E curves. We have been able to account for the presence of several channels in the experimental photochemistry of $HCo(CO)_4$ at 254 nm. We have identified the photoactive excited state and shown the absence of potential energy barrier upon dissociation. Chemiluminescence has been predicted for the photodecarbonylation reaction in the gas phase. A tentative comparison has been made of the photochemistry of $HCo(CO)_4$ and $HMn(CO)_5$. Finally, it has been proposed, on an analogy ground, that the dissociative character of the $^3A_1$ curve with respect to carbonyl loss explains the occurrence of two primary photoprocesses for $Mn_2(CO)_{10}$ at 337 nm, one of metal–metal bond cleavage and the other of dissociative loss of CO.

On the other hand, there are a number of limitations in this study, like the restriction to C_{3v} symmetry constraint and to the loss of the axial carbonyl ligand (although similar restrictions were found to be relatively unimportant in a study of the photodissociation of $Fe(CO)_5$[50]). Improving the accuracy of the calculations could be achieved by (i) carrying out a CASSCF calculation for each excited state, (ii) including some of the carbonyl orbitals (5σ, 1π, 2π) in the active space of the CASSCF calculations, and (iii) expanding the basis set to include higher spherical harmonics (mostly f functions on the metal). A complete understanding of the photochemistry of $HCo(CO)_4$, leading to an estimate of the relative quantum yields of the different photoreactions, would require the calculation of the potential energy *surfaces* as a preliminary to a study of the dynamics of the reaction. This would be justified only with the development of experimental studies in the gas phase.

Acknowledgment. The authors are grateful to Prof. P. Siegbahn of the University of Stockholm for making available the CASSCF and CCI programs. The calculations have been carried out on the CRAY-1 of the CCVR (Palaiseau) through a grant of computer time from the Conseil Scientifique du Centre de Calcul Vectoriel pour la Recherche.

Registry No. $HCo(CO)_4$, 64519-62-6.

(55) Levenson, R. A.; Gray, H. B. *J. Am. Chem. Soc.* **1975**, *97*, 6042.
(56) Kobayashi, T.; Ohtani, H.; Noda, H.; Teratani, S.; Yamazaki, H.; Yasufuku, K. *Organometallics* **1986**, *5*, 110.
(57) Prinslow, D. A.; Vaida, V. *J. Am. Chem. Soc.* **1987**, *109*, 5097.
(58) Veillard, A.; Dedieu, A. *Nouv. J. Chim.* **1983**, *7*, 683.